

Supplementary material of Satellite-based modeling of wetland methane emissions on a global scale (SatWetCH4 1.0)

Juliette Bernard^{1,2}, Marielle Saunois¹, Elodie Salmon¹, Philippe Ciais¹, Shushi Peng³, Antoine Berchet¹, Penélope Serrano-Ortiz⁴, Palingamoorthy Gnanamoorthy^{5,6}, and Joachim Jansen⁷

¹Laboratoire des Sciences du Climat et de l'Environnement, CEA-CNRS-UVSQ, Gif-sur-Yvette, France

²LERMA, Paris Observatory, CNRS, PSL, Paris, France

³College of Urban and Environmental Sciences, Peking University, Beijing 100871, China

⁴Department of Ecology, Andalusian Institute for Earth System Research (CEAMA-IISTA), University of Granada, Spain

⁵CAS Key Laboratory of Tropical Forest Ecology, Xishuangbanna Tropical Botanical Garden, Chinese Academy of Sciences, Menglun, China

⁶Coastal Systems Research, M. S. Swaminathan Research Foundation, Chennai, India

⁷Department of Ecology and Genetics/Limnology, Uppsala University, Uppsala, Sweden

Correspondence: Juliette Bernard (juliette.bernard@obspm.fr)

A Information about in situ fluxes and ancillary data

Table S1. Methane eddy covariance flux data sources

Source	Data access	Accessed
FLUX-NET CH4	https://fluxnet.org/data/fluxnet-ch4-community-product/	1 ^{rst} August 2022
AmeriFlux	https://ameriflux.lbl.gov/sites/site-search/	3 rd October 2022
EuroFlux	http://www.europe-fluxdata.eu/home/data/request-data	Novembre 2022
P. Gnanamoorthy	Personal exchanges	29 th Octobre 2022
C. Helfter	https://catalogue.ceh.ac.uk/documents/d366ed40-af8c-42be-86f2-bb90b11a659e https://catalogue.ceh.ac.uk/documents/2170ebd0-7e6f-4871-97d9-1d42e210468f	10 th October 2022

Table S2: List of methane eddy covariance flux sites used in this study

site ID	data source	lat	lon	start	end	monthly data	DOI
US-A10	FLUXNET	71.3	-156.6	2012	2018	21	https://doi.org/10.18140/FLX/1669662
US-Beo	FLUXNET	71.3	-156.6	2013	2014	16	No DOI available
US-Bes	FLUXNET	71.3	-156.6	2013	2015	27	No DOI available
US-NGB	FLUXNET	71.3	-156.6	2012	2018	39	https://doi.org/10.18140/FLX/1669687
RU-Cok	FLUXNET	70.8	147.5	2008	2016	21	https://doi.org/10.18140/FLX/1669656
US-A03	FLUXNET	70.5	-149.9	2015	2018	28	https://doi.org/10.18140/FLX/1669661
US-Atq	FLUXNET	70.5	-157.4	2013	2016	27	https://doi.org/10.18140/FLX/1669663
RU-Ch2	FLUXNET	68.6	161.4	2014	2016	26	https://doi.org/10.18140/FLX/1669654
US-ICs	AmeriFlux	68.6	-149.3	2007	2021	52	https://doi.org/10.17190/AMF/1246130
US-Ivo	FLUXNET	68.5	-155.8	2013	2016	41	https://doi.org/10.18140/FLX/1669679
SE-St1	EuroFlux	68.4	19.1	2012	2019	70	No DOI available
FI-Lom	FLUXNET	68	24.2	2006	2010	60	https://doi.org/10.18140/FLX/1669638
US-Uaf	FLUXNET	64.9	-147.9	2011	2018	48	https://doi.org/10.18140/FLX/1669701
US-NGC	FLUXNET	64.9	-163.7	2017	2018	8	https://doi.org/10.18140/FLX/1669688
US-BZF	AmeriFlux	64.7	-148.3	2011	2022	56	https://doi.org/10.17190/AMF/1756433

US-BZB	AmeriFlux	64.7	-148.3	2011	2022	59	https://doi.org/10.17190/AMF/1773401
US-BZo	AmeriFlux	64.7	-148.3	2018	2022	30	https://doi.org/10.17190/AMF/1846662
SE-Deg	EuroFlux	64.2	19.6	2014	2020	76	No DOI available
FI-Si2	FLUXNET	61.8	24.2	2012	2016	34	https://doi.org/10.18140/FLX/1669639
FI-Sii	EuroFlux	61.8	24.2	2008	2020	130	No DOI available
CA-SCB	FLUXNET	61.3	-121.3	2014	2017	30	https://doi.org/10.18140/FLX/1669613
US-KPL	AmeriFlux	60.5	-150.5	2021	2021	7	https://doi.org/10.17190/AMF/1865478
DE-Hte	FLUXNET	54.2	12.2	2011	2018	85	https://doi.org/10.18140/FLX/1669634
DE-Zrk	FLUXNET	53.9	12.9	2013	2018	63	https://doi.org/10.18140/FLX/1669636
DE-UtM	EuroFlux	52.5	8.8	2016	2017	19	No DOI available
CA-DBB	AmeriFlux	49.1	-123	2014	2020	58	https://doi.org/10.17190/AMF/1543378
CA-DB2	AmeriFlux	49.1	-123	2019	2020	13	https://doi.org/10.17190/AMF/1881564
DE-SfN	FLUXNET	47.8	11.1	2012	2014	29	https://doi.org/10.18140/FLX/1669635
US-Los	AmeriFlux	46.1	-90	2000	2022	91	https://doi.org/10.17190/AMF/1246071
US-ALQ	AmeriFlux	46	-89.6	2015	2022	35	https://doi.org/10.17190/AMF/1480323
JP-BBY	FLUXNET	43.3	141.8	2015	2018	40	https://doi.org/10.18140/FLX/1669646
US-WPT	FLUXNET	41.5	-83	2011	2013	34	https://doi.org/10.18140/FLX/1669702
US-MRM	FLUXNET	40.8	-74	2012	2013	21	No DOI available
US-ORv	FLUXNET	40	-83	2011	2015	50	https://doi.org/10.18140/FLX/1669689
US-StJ	AmeriFlux	39.1	-75.4	2014	2017	31	https://doi.org/10.17190/AMF/1480316
US-Hsm	AmeriFlux	38.2	-122	2021	2022	10	https://doi.org/10.17190/AMF/1890483
US-Srr	FLUXNET	38.2	-122	2014	2017	43	https://doi.org/10.18140/FLX/1669694
US-Tw1	AmeriFlux	38.1	-121.6	2011	2020	115	https://doi.org/10.17190/AMF/1246147
US-Tw5	AmeriFlux	38.1	-121.6	2018	2020	22	https://doi.org/10.17190/AMF/1543380
US-Tw4	AmeriFlux	38.1	-121.6	2013	2021	93	https://doi.org/10.17190/AMF/1246151
US-Myb	AmeriFlux	38	-121.8	2010	2021	133	https://doi.org/10.17190/AMF/1246139
US-Sne	FLUXNET	38	-121.8	2016	2018	32	https://doi.org/10.18140/FLX/1669693
US-EDN	AmeriFlux	37.6	-122.1	2018	2019	20	https://doi.org/10.17190/AMF/1543381
ES-Pdu	EuroFlux	37	-3.6	2014	2017	38	https://doi.org/10.1029/2019JG005169
US-NC4	AmeriFlux	35.8	-75.9	2009	2021	39	https://doi.org/10.17190/AMF/1480314
US-HB1	AmeriFlux	33.3	-79.2	2019	2021	12	https://doi.org/10.17190/AMF/1660341
US-LA2	FLUXNET	29.9	-90.3	2011	2013	22	https://doi.org/10.18140/FLX/1669681
US-LA1	FLUXNET	29.5	-90.4	2011	2012	15	https://doi.org/10.18140/FLX/1669680

US-DPW	FLUXNET	28.1	-81.4	2013	2017	40	https://doi.org/10.18140/FLX/1669672
HK-MPM	FLUXNET	22.5	114	2016	2018	34	https://doi.org/10.18140/FLX/1669642
IN-Pic	P. Gnanamoorthy	11.4	79.8	2018	2020	8	No DOI available
MY-MLM	FLUXNET	1.5	111.1	2014	2015	19	https://doi.org/10.18140/FLX/1669650
ID-Pag	FLUXNET	-2.3	113.9	2016	2017	12	https://doi.org/10.18140/FLX/1669643
PE-QFR	AmeriFlux	-3.8	-73.3	2018	2019	10	https://doi.org/10.17190/AMF/1671889
BR-Npw	FLUXNET	-16.5	-56.4	2013	2016	30	https://doi.org/10.18140/FLX/1669368
BW-Gum	C. Helfter	-19	22.4	2018	2020	26	https://doi.org/10.5285/d366ed40-af8c-42be-86f2-bb90b11a659e
BW-Nxr	C. Helfter	-19.5	23.2	2018	2020	12	https://doi.org/10.5285/2170ebd0-7e6f-4871-97d9-1d42e210468f
NZ-Kop	FLUXNET	-37.4	175.6	2012	2015	48	https://doi.org/10.18140/FLX/1669652

B Comparison of ERA5 data with in situ data

B.1 Temperature

We study the variable *Soil temperature level 2 (lay2)* from ERA5, which represents soil temperature in 7-28 cm soil layer.

5 We compare it to soil temperature measurements available at the sites. Out of the 58 sites, 42 are equipped with temperature probes. If multiple probes are available, we choose the one closest to the surface. For ERA5, we select the nearest pixel to the site.

ERA5 *lay2* temperature is consistent with in situ measurements. The comparison is shown in Fig.S1. Each site is represented by a point. In Fig.S1.a., the temporal correlation between ERA5 temperature and observations is strong: r is bigger than 0.9 for 37 out of 42 sites. A RMSD lower than 2 °K is shown for 39 out of 42 sites on Fig.S1.b. ERA5 temperatures have a good spatial correlation on average with observations, as Fig.S1.c. shows a linear relationship between mean in situ temperatures and mean ERA5 *lay2* temperatures. There is an RMSD of 1.8 °K between the observation and ERA5 means. Finally, Fig.S1.d. indicates a good reproduction of the seasonal variations for ERA5 *lay2*: the RMSD between the sites standard deviations of observations and ERA5 is 1.2 °K.

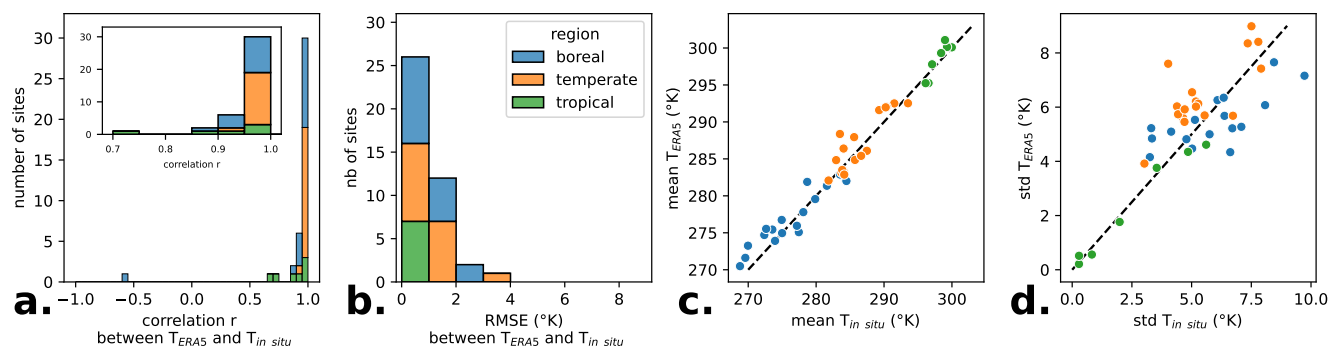


Figure S1. Comparison of 0.25° ERA5 *lay2* temperature with in situ temperature measurements. ERA5 data consistently match local in situ measurements. Each point represents a site. **a.** Temporal correlation coefficient between ERA5 *lay2* temperature and in situ data. **b.** RMSD of ERA5 data compared to observations. **c.** Spatial pattern: mean in situ temperature for each site compared to mean of ERA5 estimates. **d.** Amplitude comparison: standard deviation of in situ temperature for each site compared to standard deviation of ERA5 estimates.

15 B.2 Soil Water Content (SWC)

We study the variable *SWC level 2* from ERA5, which represents Soil Water Content (SWC) in 7-28 cm soil layer. We compare it to SWC measurements available at the sites. Out of the 58 sites, 14 are equipped with SWC probes. For ERA5, we select the nearest pixel to the site.

ERA5 SWC 0.25° data do not consistently match local in situ measurements. Indeed, Fig.S2.a. shows an unclear temporal correlation between in situ SWC and ERA5 SWC. Fig.S2.b. indicates high RMSDs (0-30% for values around 40%) between

ERA5 and local SWC measurements. Moreover, ERA5 tends to underestimate the mean SWC compared to local measurements as shown in Fig.S2.c. ERA5 highlights a significant underestimation of SWC variation amplitude by ERA5 compared to observations (Fig.S2.d.).

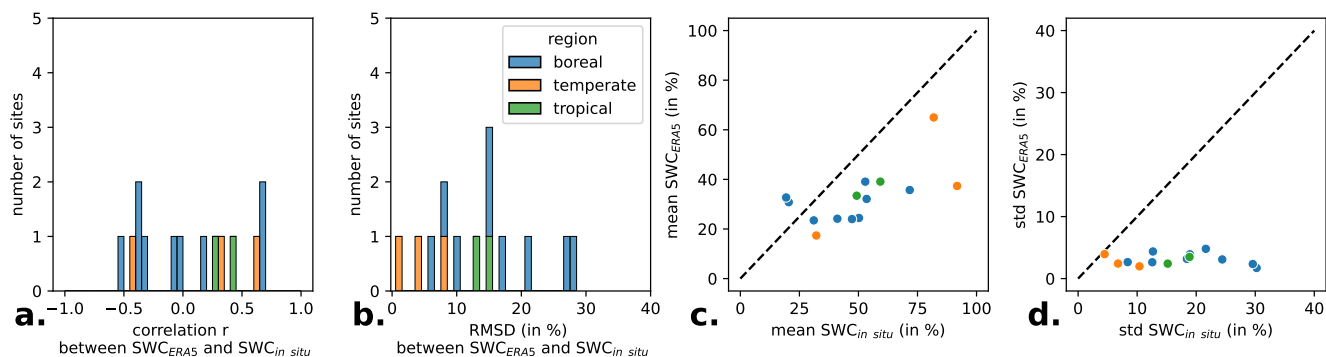


Figure S2. Comparison of 0.25° lay2 ERA5 Soil Water Content (SWC) with local in situ SWC observations. ERA5 data does not consistently match local in situ measurements. Each point represents a site. **a.** Temporal correlation between in situ SWC and ERA5 SWC. **b.** RMSD between ERA5 SWC and observed local SWC. **c.** Spatial pattern: mean in situ SWC for each site compared to mean of ERA5 SWC. **d.** Amplitude comparison: standard deviation of in situ SWC for each site compared to standard deviation of ERA5 estimates.

C Land surface models detailed outputs

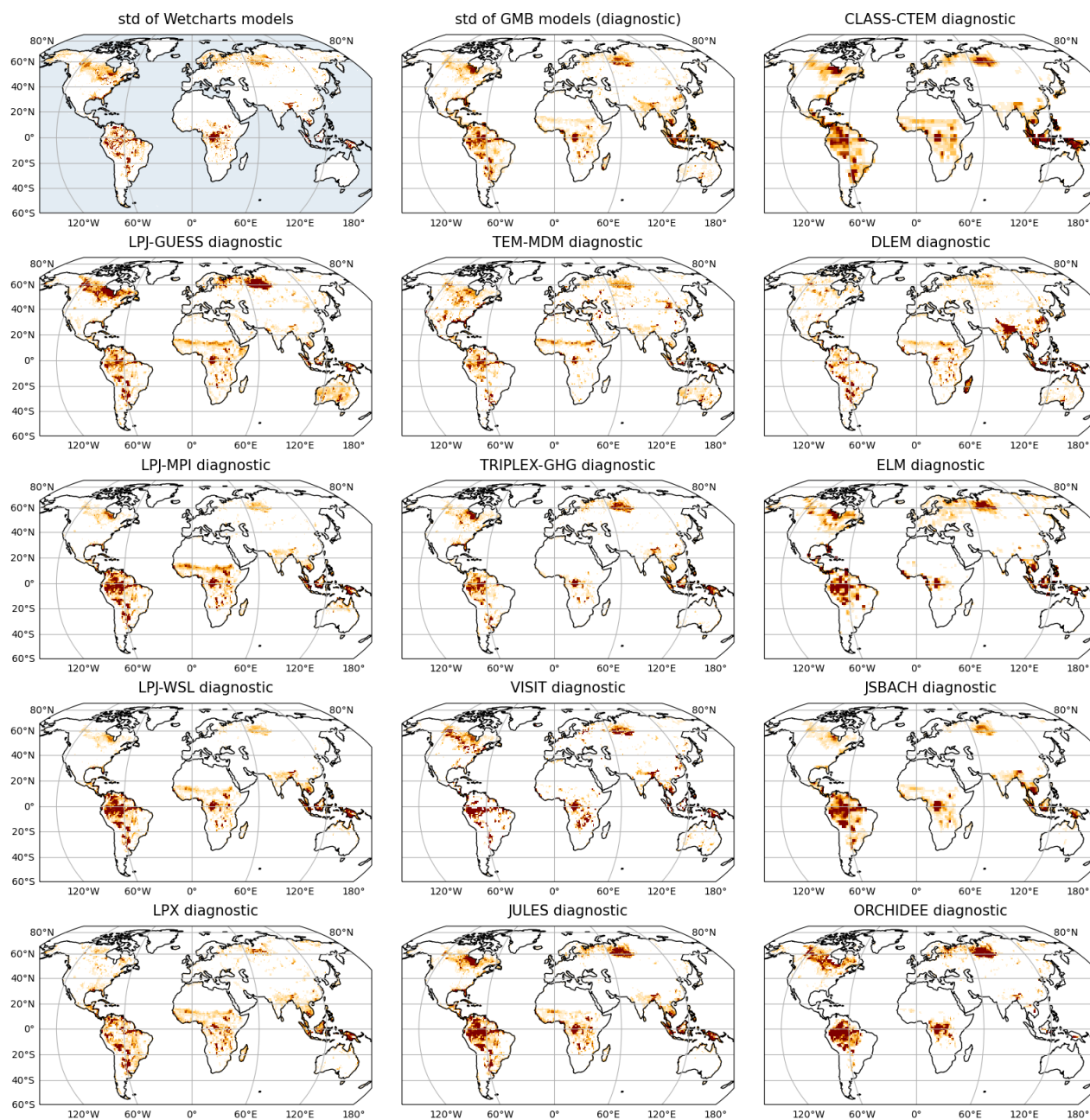


Figure S3. Emissions monthly mean for 2003-2018 of Land surface Models run with WAD2M for GMB (Sauniois et al., 2020). Spatial patterns and intensity show considerable variability between the different GMB Land Surface Models, especially in Canada, subequatorial Africa, Siberian Lowland, and Australia.

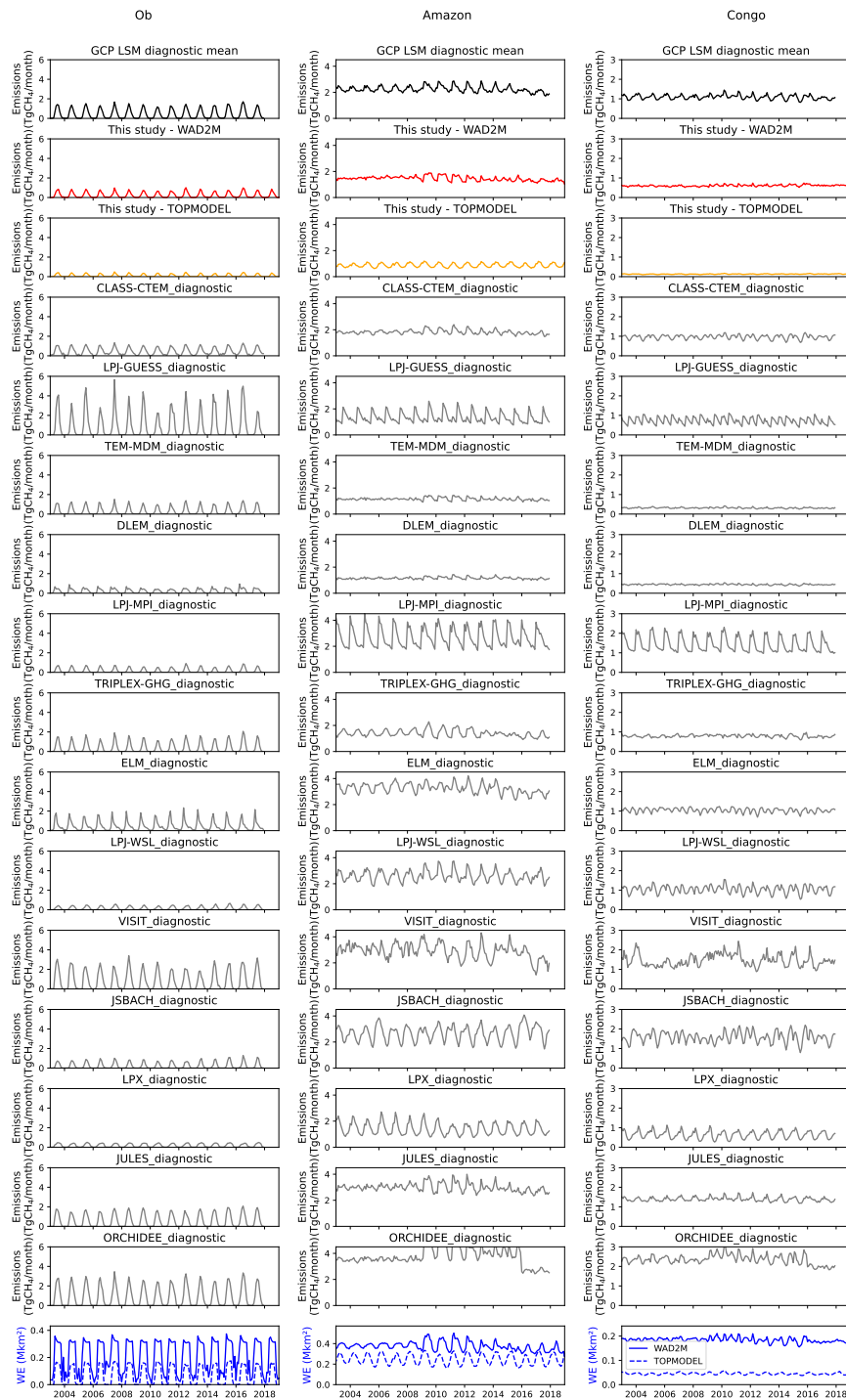


Figure S4. Methane emissions from different basins (Ob, Amazon and Congo) from the mean of the GMB LSM models diagnostic (black), our simulations (red), and each LSM from GMB diagnostic runs (grey). The Wetland Extent (WE) used for the runs is WAD2M and is shown in the lower graphs.

25 **References**

- Saunois, M., Stavert, A. R., Poulter, B., Bousquet, P., Canadell, J. G., Jackson, R. B., Raymond, P. A., Dlugokencky, E. J., Houweling, S., Patra, P. K., Ciais, P., Arora, V. K., Bastviken, D., Bergamaschi, P., Blake, D. R., Brailsford, G., Bruhwiler, L., Carlson, K. M., Carrol, M., Castaldi, S., Chandra, N., Crevoisier, C., Crill, P. M., Covey, K., Curry, C. L., Etiope, G., Frankenberg, C., Gedney, N., Hegglin, M. I., Höglund-Isaksson, L., Hugelius, G., Ishizawa, M., Ito, A., Janssens-Maenhout, G., Jensen, K. M., Joos, F., Kleinen, T., Krummel, P. B., Langenfelds, R. L., Laruelle, G. G., Liu, L., Machida, T., Maksyutov, S., McDonald, K. C., McNorton, J., Miller, P. A., Melton, J. R., Morino, I., Müller, J., Murguia-Flores, F., Naik, V., Niwa, Y., Noce, S., O'Doherty, S., Parker, R. J., Peng, C., Peng, S., Peters, G. P., Prigent, C., Prinn, R., Ramonet, M., Regnier, P., Riley, W. J., Rosentreter, J. A., Segers, A., Simpson, I. J., Shi, H., Smith, S. J., Steele, L. P., Thornton, B. F., Tian, H., Tohjima, Y., Tubiello, F. N., Tsuruta, A., Viovy, N., Voulgarakis, A., Weber, T. S., van Weele, M., van der Werf, G. R., Weiss, R. F., Worthy, D., Wunch, D., Yin, Y., Yoshida, Y., Zhang, W., Zhang, Z., Zhao, Y., Zheng, B., Zhu, Q., Zhu, Q., and Zhuang, Q.: The Global Methane Budget 2000–2017, *Earth System Science Data*, 12, 1561–1623, <https://doi.org/10.5194/essd-12-1561-2020>, 2020.